Temperature and pressure dependence of the dynamics in a poly(methyl acrylate) side-chain liquid-crystalline polymer

G. Floudas*
University of Ioannina, Department of Physics, P.O. Box 1186, 451 10 Ioannina, Greece
and Foundation for Research and Technology-Hellas (FORTH)-Biomedical Research Institute (BRI), Ioannina, Greece

M. Mierzwa
Max-Planck Institut für Polymerforschung, Postfach 3148, D-55021 Mainz, Germany
and Institute of Physics, Silesian University 40-007 Katowice, Poland

A. Schönhals
Bundesanstalt für Materialforschung und-prüfung, Unter den Eichen 87, D-12205 Berlin, Germany
(Received 22 October 2002; published 24 March 2003)

The molecular dynamics of a side-chain polymer liquid crystal with a poly(methyl acrylate) backbone and a (*p*-alkoxy-phenyl)-benzoate mesogenic group have been studied in the unaligned state as a function of temperature and pressure using dielectric spectroscopy. Polarizing optical microscopy, differential scanning calorimetry, and pressure-volume-temperature (PVT) measurements revealed three transition temperatures separating four phases (glass, smectic, nematic, and isotropic). Different dynamic processes have been identified reflecting librational modes (γ process), local relaxation of the mesogenic group (β process), the segmental mode (α process) associated with the dynamic glass transition, and a slower process (δ process) reflecting the side-chain dynamics within the liquid crystal order. Pressure exerts a stronger influence on the α as compared to the δ process. Starting from the nematic phase, pressure was found to induce the nematic-to-smectic transformation. The associated dynamic changes were in excellent agreement with the PVT results implying that the dynamics are directly coupled to the thermodynamic state. Pressure was found to enhance the stability of the smectic order within the *P-T* phase diagram.

DOI: 10.1103/PhysRevE.67.031705 PACS number(s): 64.70.Md, 61.41.+e, 77.84.Nh

I. INTRODUCTION

Thermotropic polymer liquid crystals are hybrid materials that exhibit similar mesophases characteristic of ordinary liquid crystals, yet retain the useful and versatile properties of polymers. Among the different polymer liquid crystals, side-chain polymer liquid crystals are by far the most promising [1,2]. Side-chain polymer liquid crystals, where the mesogen unit is attached on the side chain of a polymer backbone, have attracted a lot of attention because of their commercial applications ranging from high strength materials such as fibers to optical nonlinear devices including waveguides and electro-optic modulators in poled polymeric slab wave guides. A key point for the use of polymer liquid crystals in the display industry is the response time to an external electric field that is determined by the reorientational dynamics of the polymer backbone and of the mesogen.

This requirement motivated several investigation of the dynamics in thermotropic side-chain polymer liquid crystals mainly by dielectric spectroscopy (*DS*) and *NMR* [3–15]. Temperature, however, is not the only determining factor. Pressure, based on simple thermodynamics, should also affect the mesoscopic structure but, until now, a complete phase diagram for polymer liquid crystals is missing.

There have been three reports on the effect of applied pressure on the dynamics of liquid crystalline polymers. The first was on unaligned polyacrylates with *p*-cyano-phenyl benzoate side group forming a nematic phase [11]. The dielectric measurements were made for some temperatures in the range from 323 to 413 K, for frequencies in the range 10^{-2} to 10^{6} Hz and for pressures up to 5 kbar. It was found that pressure can induce an isotropic-to-nematic transition with a dT_{NI}/dP of 40 K/kbar. Furthermore, from the two relaxation processes identified as α and δ relaxation, the latter was found to be less affected by pressure and thus less volume demanding. The second study [12] dealt with a side-chain liquid crystalline polysiloxane, studied in the temperature range from 323 to 358 K, for frequencies in the range from 10 to 10^{5} Hz and for pressures up to 1.5 kbar. Two relaxation processes have been identified, discussed as α and δ process, with the latter showing much narrower width. The fact that the δ process had a width close to a single relaxation time process was discussed as revealing a different mechanism for motion as compared to the more cooperative α process. The third study [13] was made on two unaligned derivatives (called $H3$ and $H9$) of poly(norbornene diethylester) with different spacer lengths (3 and 9) giving rise to a nematic and a smectic mesophase, respectively. Measurements were made in the temperature range from 190 to 433 K, for frequencies in the range from 10^{-2} to 10^{9} Hz and for pressures up to 3 kbar. It was shown that the segmental (α) process reflects the dynamic glass transition and that the slower (δ) process, observed only in the polymer with the longer spacer length ($H9$), reflects the side-chain dynamics within the smectic layers. The possibility of com-

*Corresponding author. Email address: gfloudas@cc.uoi.gr

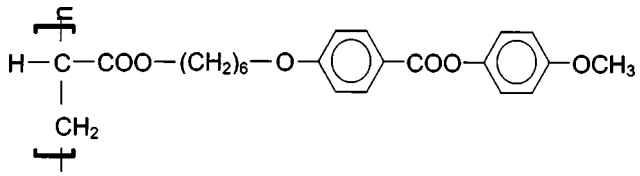

FIG. 1. Schematic of the structure of the side-chain polymer liquid crystal.

plete reorientation of the mesogen around the backbone was excluded as a dynamic process due to the double bonds in the norbornene backbone that restrict such a motion. In addition, it was shown that the two modes merge by decreasing temperature and by increasing pressure, suggesting a common origin under conditions of low T and/or high compression.

In the present study we employ a side-chain liquid crystalline polymer, composed from a (*p*-alkoxy-phenyl)-benzoate side chain linked to a poly(alkyl acrylate) backbone by six methylene spacer units exhibiting multiple mesophases and investigate the effect of temperature and pressure on inducing phase transformations. Our aim is to construct a *P-T* phase diagram and to investigate the stability of the different ordered mesophases. Furthermore, we investigate how the dynamic processes are coupled to the thermodynamic state of the system. For this purpose we employ both ''static'' [i.e., pressure-volume-temperature (PVT), differential scanning calorimetry (DSC)] as well as dynamic probes (i.e., dielectric spectroscopy). We found that there is a nice correspondence between the thermodynamic state and the associated dynamics.

II. EXPERIMENT

The structure of the polymer is shown in Fig. 1. The weight- and number-averaged molecular weights were 13 500 and 5900 g/mol, respectively. Details on the synthesis and chemical characterization can be found in Refs. [16,17].

A Zeiss polarizing optical microscope was used together with a Linkam heating stage (*THMS* 600) with temperature programmer. The experiments were made by heating to an initial temperature ($T=410$ K) corresponding to the isotropic state followed by subsequent cooling to temperatures corresponding to the liquid crystalline structures. Subsequently images were taken corresponding to the smectic ($T=366$ K) and nematic ($T=393$ K) regimes. Representative optical microscopy images are shown in Fig. 2 with textures exhibiting a smectic (x rays identified a smectic *A* mesophase) and a nematic mesophase, respectively.

A Mettler Toledo Star DSC capable of programmed cyclic temperature runs over the range 113–673 K was used. Samples were first heated with a rate of 10 K/min to temperatures corresponding to the isotropic state and subsequently cooled to 273 K with the same rate. The experiment was repeated with a rate of 5 K/min and the results for the transition temperatures and enthalpies obtained with the lowest rate (5 K/min) are summarized in Table I. Typical DSC traces are shown in Fig. 3 (top) on cooling and subsequent

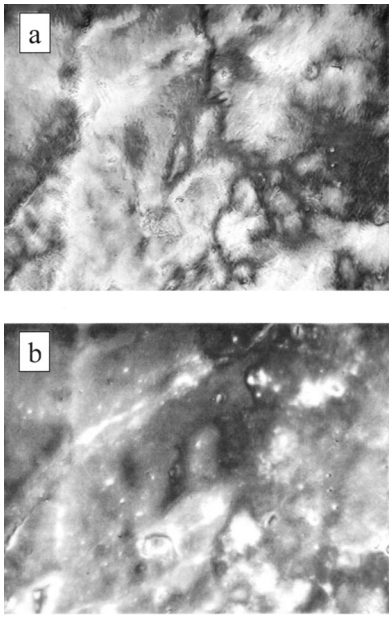

FIG. 2. Optical micrographs taken at 366 K (top) and 393 K (bottom) corresponding to the smectic and nematic phases, respectively. The size of the micrographs is 200 μm $\times$ 150 μm.

heating. Two exothermic peaks exist on cooling followed by a glass transition. On heating, the glass temperature is located at 300 K (with a heat capacity step of $\Delta c_p = 0.6$ J/g K) followed by two endothermic peaks at 370 K ($\Delta H = 2.5$ J/g) and at 397 K ($\Delta H = 2.6$ J/g) corresponding to the smectic-to-nematic (*SN*) and nematic-to-isotropic (*NI*) transitions, respectively.

The pressure-volume-temperature (PVT) measurements were made using a fully automated *GNOMIX* high-pressure dilatometer. The powder material was modeled at 473 K prior to the measurements and about 1 g was used in the measurements. We first performed runs by changing pressures from 10 to 200 MPa (1 MPa = 0.01 kbar) in steps of 10 MPa at constant temperatures (i.e., under ''isothermal'' conditions) from 300 to 473 K. Subsequently, measurements were made by heating/cooling experiments with a rate of 1 K/min at different fixed pressures (i.e., under ''isobaric'' conditions) in the range from 10 to 100 MPa. The result from the ''isothermal'' measurements is shown in Fig. 3 at some pressures.

The setup for the pressure dependent dielectric measurements consisted of the following parts (described elsewhere in detail): temperature controlled sample cell, hydraulic closing press with pump, and a pump for hydrostatic test pressure. Silicon oil was used as the pressure transducing me-

TABLE I. Molecular characteristics and transition temperatures.

Sample	M_w	M_n	T_g (K)	$T_{\text{transition}}$ (K)	ΔH (J/g)
PA6	13500	5900	300	$S \xrightarrow{370\ \text{K}} N$	2.5
				$N \xrightarrow{397\ \text{K}} I$	2.6

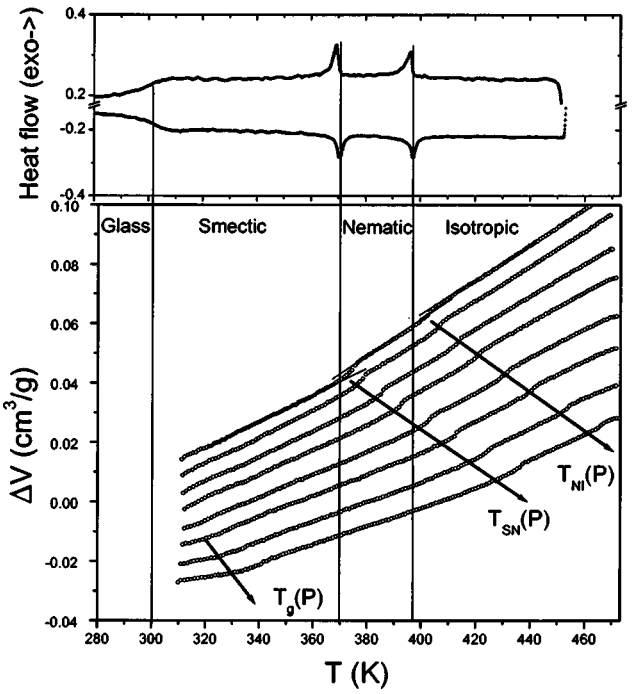

FIG. 3. (Top) DSC trace of the polymer taken on cooling and subsequent heating (with a rate of 10 K/min) indicating a glass transition at 300 K, a smectic-to-nematic transition at about 370 K and a nematic-to-isotropic transition at 397 K. The transition temperatures are indicated by vertical lines. (Bottom) Relative change in the specific volume (ΔV) as a function of temperature for different pressures in the range from 10 to 200 MPa. The data were obtained under ''isothermal'' conditions. The lines through the 10 MPa data points are guides to the eye. The arrows indicate the pressure dependence of the glass temperature (T_g), of the smectic-to-nematic transition (T_{SN}), and of the nematic-to-isotropic transition (T_{NI}). Notice the steeper dependencies of the first order transitions as opposed to the glass temperature. These dependencies are discussed in more detail with respect to Fig. 10.

dium. The sample cell consisted of two electrodes of 20 mm diameter and a sample with a thickness of 50 μm. The sample capacitor was sealed and placed inside a teflon ring to separate the sample from the silicon oil. The dielectric measurements were made at different temperatures in the range 163 to 413 K, for pressures in the range from 1 bar to 3 kbar, and for frequencies in the range from 10^{-2} to 10^{6} Hz using a Novocontrol BDS system composed from a frequency response analyzer (Solartron Schlumberger FRA 1260) and a broad band dielectric converter. Measurements in the frequency range from 10^{6} to 10^{9} Hz were made with a coaxial reflectometer based on the *HP*4191 impedance analyzer.

The complex dielectric permittivity $\varepsilon^*=\varepsilon'-i\varepsilon''$, where ε' is the real and ε'' is the imaginary part, is a function of frequency ω, temperature T and pressure P, $\varepsilon^*=\varepsilon^*(\omega,T,P)$. In Fig. 4, some representative dielectric loss spectra are shown under isobaric ($P=1$ bar) and isothermal ($T=363$ K) conditions. The spectra reveal multiple relaxation processes which are indicated with the Greek letters β, α, and δ by increasing temperature. In the analysis of all DS spectra we have used the empirical equation of Havriliak and Negami (HN) [18]

$$\frac{\varepsilon^*(T,P,\omega)-\varepsilon_\infty(T,P)}{\Delta\varepsilon(T,P)}=\frac{1}{\{1+[i\omega\tau_{\mathrm{HN}}(T,P)]^{\alpha}\}^{\gamma}}, \quad (1)$$

where $\tau_{\mathrm{HN}}(T,P)$ is the characteristic relaxation time in this equation, $\Delta\varepsilon(T,P)=\varepsilon_s(T,P)-\varepsilon_\infty(T,P)$ is the relaxation strength of the process under investigation, and α, γ describe, respectively, the symmetrical and asymmetrical broadening of the distribution of relaxation times. In the fitting procedure we have used the ε'' values at every temperature and pressure and in some cases the ε' data were also used as a consistency check. The linear rise of the ε'' at lower frequencies is caused by the conductivity [ε''

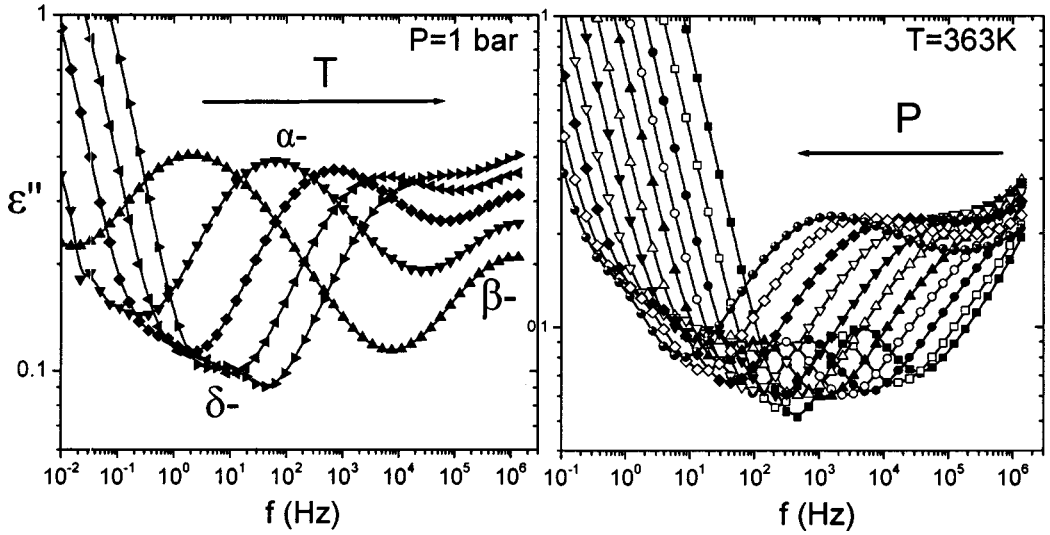

FIG. 4. Dielectric loss spectra plotted (left) at atmospheric pressure for different temperatures [(▲): $T=303$ K, (▼): $T=308$ K, (♦): $T=313$ K, (◀): $T=318$ K, (▶): $T=323$ K] and (right) at 363 K for different pressures [(■): $P=0.1$ kbar, (□): $P=0.3$ kbar, (●): $P=0.6$ kbar, (○): $P=0.9$ kbar, (▲): 1.2 kbar, (△): $P=1.5$ kbar, (▼): $P=1.8$ kbar, (▽): $P=2.1$ kbar, (♦): $P=2.4$ kbar, (◇): $P=2.7$ kbar, (●): $P=2.9$ kbar].

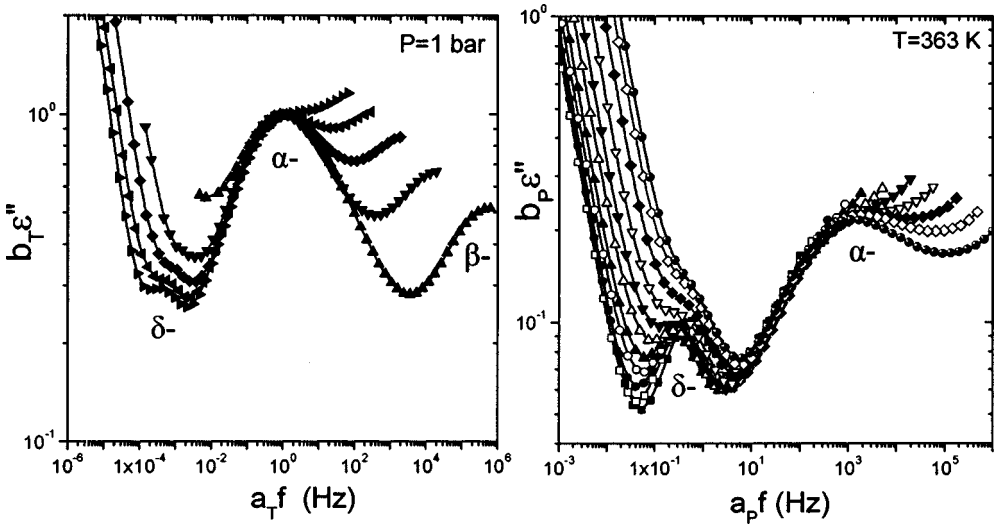

FIG. 5. ''Master-curve'' construction of the isobaric (left) and the isothermal (right) spectra using the same data as in Fig. 4 shifted to the corresponding reference spectrum. The reference spectra were at $T=303$ K and $P=2.9$ kbar for the isobaric and isothermal experiments, respectively.

$\sim(\sigma_0/\varepsilon_0)\omega^{-1}$, where σ_0 is the dc conductivity and ε_0 is the permittivity of free space] which has been included in the fitting procedure.

III. RESULTS AND DISCUSSION

The results from the polarizing optical microscopy (Fig. 2) indicated a change of the mesoscopic structure at approximately 370 K that could imply a transition from a smectic to a nematic order. In addition, the isotropization temperature was found at about 400 K. The same transitions affect the DSC trace on cooling and subsequent heating (Fig. 3). Two first-order transitions have been identified on heating, at 370 and 397 K, associated with the smectic-to-nematic and nematic-to-isotropic transitions, respectively. In addition, a glass transition has been identified at lower temperatures ($T_g=300$ K). Another direct evidence of the nature of the transitions in PA6 is provided by the *PVT* measurements also shown in Fig. 3. Figure 3, depicts the relative volume change (ΔV) as a function of temperature for different pressures in the range from 10 to 200 MPa. Notice the change of slope associated with the glass temperature and, at higher temperatures, the two first-order transitions accompanied by a stepwise increase in specific volume. The effect of compression on the three temperatures is very distinct. As expected, pressure affects the glass temperature to a lesser extent as compared to the first-order transitions at higher temperatures (see the discussion with respect to Fig. 10). Thus, polarizing optical microscopy, DSC and *PVT* results revealed the existence of considerable mesoscopic order as well as transitions between the different liquid crystalline phases. In addition, DSC and *PVT*, identified a temperature of structural arrest (T_g). These ''static'' thermodynamic properties will be compared with the associated dynamic changes, below.

DS: temperature dependence. The DS results, performed over a broad frequency, *T* and *P* ranges are discussed next. The effect of *T* on the dielectric loss spectra at atmospheric pressure (i.e., under ''isobaric'' conditions) are compared with the corresponding spectra at 363 K (i.e., under ''isothermal'' conditions) by changing pressure in Fig. 4. Three dynamic processes affect the loss spectra within the *T* and *P* ranges shown in Fig. 4. Starting from higher frequencies, the ''fast'' β process is followed by the intermediate α process and at lower frequencies by the δ process. Two additional processes were found (which are not shown in Fig. 4 for clarity reasons): a γ process at even lower temperatures and another slower process under conditions of high *T* and low *P* (Maxwell-Wagner polarization, see below). For the three processes shown in Fig. 4, increasing *T* results in a strong shift of the α and δ processes to higher frequencies and to a smaller shift on the β process. The effect of increasing *P* is, qualitatively, similar to decreasing *T*, that is, all processes become slower but the α and δ processes are again more affected. Increasing pressure, however, has more functions than just decreasing temperature. The modes become more intense due to the densification (α process) and due to improved order (δ process). Furthermore, as a result of the improved order, pressure can stabilize certain mesophases (see below).

We attempted to construct master curves by shifting each curve of Fig. 4 to the α process maximum loss at a reference *T* and *P*, by multiplying the frequency axis of each curve by appropriate shift factors a_T and a_P at each *T* and *P*. The result of the attempted time-temperature superposition (*tTs*) and time-pressure superposition (*tPs*) is shown in Fig. 5 and reveal that *tTs* and *tPs* fail over a broad *f-T-P* range. Small vertical shifts (with factors b_T and b_P) were also required. The failure of *tTs* and *tPs* reveals that the three processes have different *T* and *P* dependencies involving different apparent activation energies or apparent activation volumes (see text below).

The results from the HN fit to the relaxation times at maximum loss for each process are depicted in Fig. 6. Two

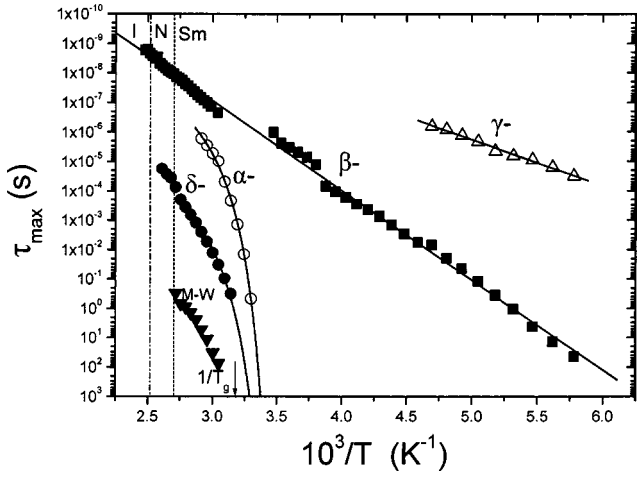

FIG. 6. Arrhenius representation of the relaxation times for the different processes: (△) γ process, (■) β process, (○) α process, (●) δ process and the process corresponding to the Maxwell-Wagner polarization (▼). The vertical lines correspond to the nematic-to-isotropic and smectic-to-nematic transitions.

processes (β and γ) with an Arrhenius T dependence exist at lower temperatures that can be described as

$$\log_{10}\tau_{\max}=\log_{10}\tau_0+\frac{E}{2.303RT}, \tag{2}$$

where τ_0 is the relaxation time at practically infinite temperature and E is the activation energy. The γ process, with an activation energy of 7.2 kcal/mol and with a constant, albeit low, dielectric strength of $T\Delta\varepsilon\sim 30$ reflects a very localized librational motion of the side chain. The β process, studied here over 11 decades in frequency, has an activation energy of 14.6 kcal/mol and dielectric strength which varies with T from a $T\Delta\varepsilon$ value of 100 at low T to about 300 at higher T suggesting the unfreezing of dipoles with increasing T. Earlier NMR investigations [19] on a similar sample with a deuterated phenyl ring on the phenylbenzoate mesogenic group identified a β process operating on comparable time scales related to π flips of the phenyl ring. Such a process would be dielectrically inactive but the similarity in the time scales of the two processes could suggest a concerted motion of the ester and phenyl ring within the mesogenic unit as responsible for the β process.

At higher temperatures, the two processes named α and δ, have distinctly different T dependence, when compared to the processes at lower T, that conform to the Vogel-Fulcher-Tammann (VFT) equation

$$\log_{10}\tau_{\max}=\log_{10}\tau_0+\frac{B}{T-T_0}, \tag{3}$$

where B is the apparent activation energy and T_0 ($=278.6$ K) is the ''ideal'' glass transition temperature located 21 K below the calorimetric T_g. We should mention here that due to the small frequency range for the slower δ process the T_0 value was kept fixed to the corresponding value from the α process. This corroborates the notion that the two processes will freeze at the same temperature as was found in a recent study of the dynamics of another side-chain liquid crystalline polymer [i.e., poly(norbornene diethylester)]. It has been discussed earlier, that the α and δ processes reflect the dynamic glass transition and a local reorientation of the mesogen within the LC layers. The parameters of all processes are summarized in Table II. Notice that at higher frequencies a single—albeit broad—dielectrically active process was found whose location lies in the extrapolation from the low temperature β process. However, within this frequency range, the rate of the slower α-process approaches the rate of the faster β process, thus making the deconvolution of the two processes a very difficult task. A slower process with very high intensity which can not have molecular origin was also identified which associates with the Maxwell-Wagner (MW) polarization mechanism due to the locally inhomogeneous environment.

TABLE II. Activation parameters for the different relaxation processes.

PA6	δ	α	β	γ
$\log(\tau_0/s)$	-6.4	9.2	-16.8	-13.6
E (kcal/mol)			14.6	7.2
B (K)	237 ± 8	218 ± 26		
T_0 (K)	278.6[a]	278.6 ± 2		

[a]Value held fixed.

Most of the relaxation times of Fig. 6 are reported for temperatures within the smectic mesophase and only the β and δ processes were followed within the nematic phase. The effect of the smectic-to-nematic transition on the length scale of the β process is insignificant due to the local character of the process that is unaffected by the loss of translational order. In contrast, the more cooperative δ process is affected by the transition becoming faster as a result of the change in local friction.

DS: pressure dependence. Pressure is an additional thermodynamic variable that affects the dynamic processes (Fig. 4) [20–29]. For example, pressure was helpful in the study of the dynamics in type-A polymers [21,22], in polymer blends and block copolymers [23,20], as well as in studying the process of crystallization [24] and the associated kinetics [25] in semicrystalline polymers. The pressure dependence of the relaxation times corresponding to the maximum loss for the α and δ processes is shown in Fig. 7. Notice the different response to pressure for the two processes: a linear pressure dependence for the δ process and a strongly nonlinear dependence for the α process. The linear dependence for the δ process can have different origins. Transition state theory [20] predicts

$$\Delta V=RT\left(\frac{\partial\ln\tau}{\partial P}\right)_T, \tag{4}$$

where ΔV is the difference in the molar volumes of activated and nonactivated species. In addition, free volume theory [20] results in the same equation assuming the exponential

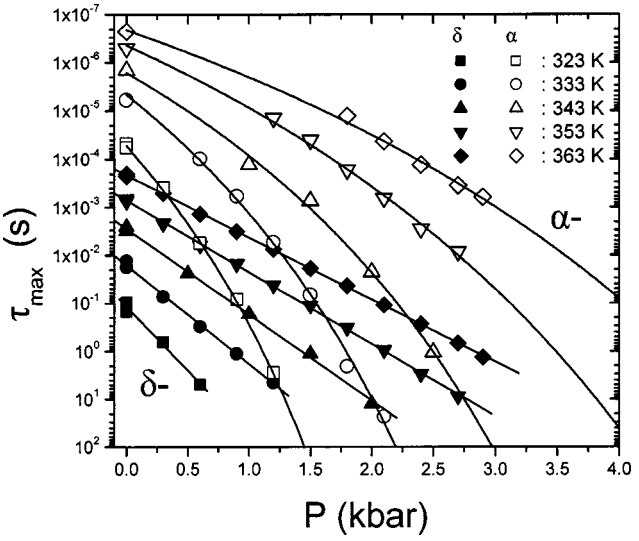

FIG. 7. Pressure dependence of the relaxation times corresponding to the maximum loss for the α (open symbols) and δ (filled symbols) processes at different temperatures as indicated. The lines are fits to different equations (see text).

model, which results in a linear dependence of the logarithm of shift factors a_P, defined as the ratio of the relaxation times τ_P at pressure P to the corresponding value at a reference pressure P_0,

$$\ln a_P = \Lambda(P - P_0). \tag{5}$$

In the above equation, Λ is independent of pressure and because of the similarity of Eq. (4) to (5), the coefficient Λ is interpreted also as an apparent activation volume, i.e., $\Lambda = \Delta V/RT$. The shortcomings of the free volume approach have been discussed in the literature. The linear pressure dependence for the δ process shown in the Fig. 7, results in an apparent activation volume ranging from 160 to 90 cm^3/mol within the T range from 323 to 363 K. In contrast, the P dependence for the α process can be parametrized according to

$$\tau_{\max} = \tau_\alpha \exp\left(\frac{DP}{P_0 - P}\right), \tag{6}$$

where τ_α is the segmental relaxation time at atmospheric pressure at the given temperature, P_0 is the pressure corresponding to the ideal glass transition, and D is a dimensionless parameter. The lines through the data points corresponding to the α process in Fig. 7 are the result of the fit to Eq. (6). Notice, that there exists a finite pressure (P_x) at the corresponding temperature (T_x), obtained by extrapolation, where the two processes merge.

The universality of Eq. (6) can be tested by plotting the reduced relaxation times as a function of reduced pressure. This is shown in Fig. 8 and results in a reasonable linearity with a zero extrapolation. We mention here that the scaling of the α process shown in the figure represents relaxation times obtained within the temperature range from 323 to 363 K, that is, solely within the smectic mesophase.

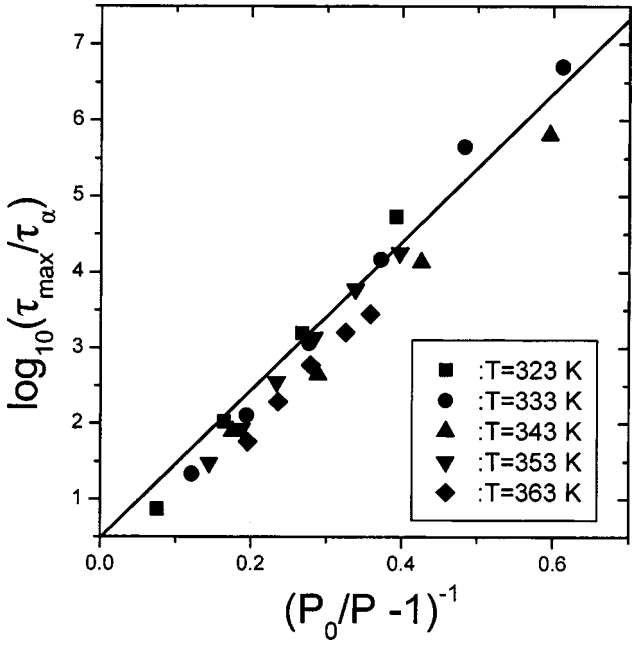

FIG. 8. Pressure dependence of the normalized relaxation times of the α process as a function of reduced pressure for five temperatures as indicated. The line is only a guide to the eye.

In addition, pressure can affect the mesophases by inducing order-to-order or disorder-to-order transitions as already shown by the PVT results (Fig. 3). For example, based on PVT, we can anticipate that compressing the nematic phase will result in a nematic-to-smectic transformation. Figure 9

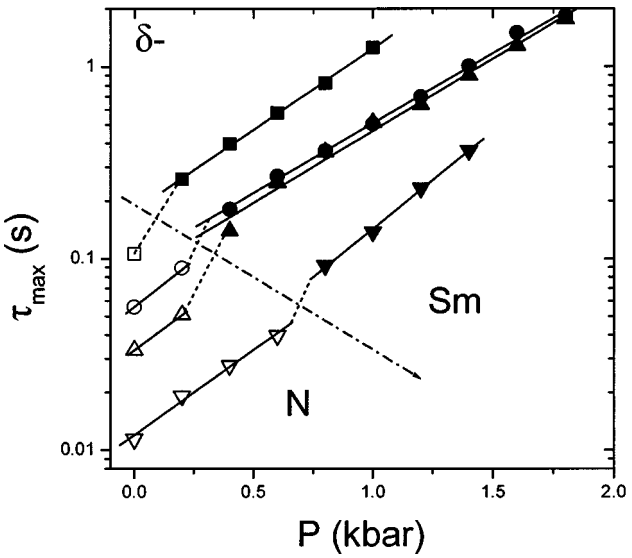

FIG. 9. Pressure dependence of the relaxation times of the δ process at four temperatures. Squares: $T = 368$ K, circles: $T = 373$ K, up triangles: $T = 378$ K, and down triangles: $T = 388$ K. The open and filled symbols correspond to data obtained in the nematic and smectic mesophases, respectively. Notice the slower relaxation within the smectic mesophase as compared to the nematic phase. The line gives the dependence of the δ process relaxation times on pressure at the nematic-to-smectic transition, resulting in a dP/dT of 0.035 kbar/K.

TABLE III. Calculated change of specific volume (ΔV) from the Clausius-Clapeyron equation.

Transition	dT/dP (K/kbar)	$\Delta V(10^{-3}$ cm^3/g)
$S \xrightarrow{370\ \mathrm{K}} N$ (DS)	32±4	2.1±0.8
$S \xrightarrow{370\ \mathrm{K}} N$ (PVT)	31.4±0.8	2.0±0.5
$N \xrightarrow{397\ \mathrm{K}} I$ (PVT)	33.2±0.9	2.0±0.5

depicts the change of the relaxation times at maximum loss by pressurization of the δ process in going from the nematic (open symbols) to the smectic (filled symbols) mesophase. Notice that the effect of the mesophase transformation on the dynamics is to slow-down the relaxation times by a factor of 2. The slower dynamics within the smectic mesophase can be understood in terms of the higher translational order that restricts the reorientational motion of the mesogen. The resulted dP/dT dependence (arrow in Fig. 9) of 0.035 kbar/K is in good agreement with the PVT results (see Table III below). Furthermore, the linear pressure dependence of the logarithm of the relaxation times at a given T is preserved in the induced smectic mesophase with a similar apparent activation volume as in the nematic phase implying essentially the same molecular mechanism in both mesophases.

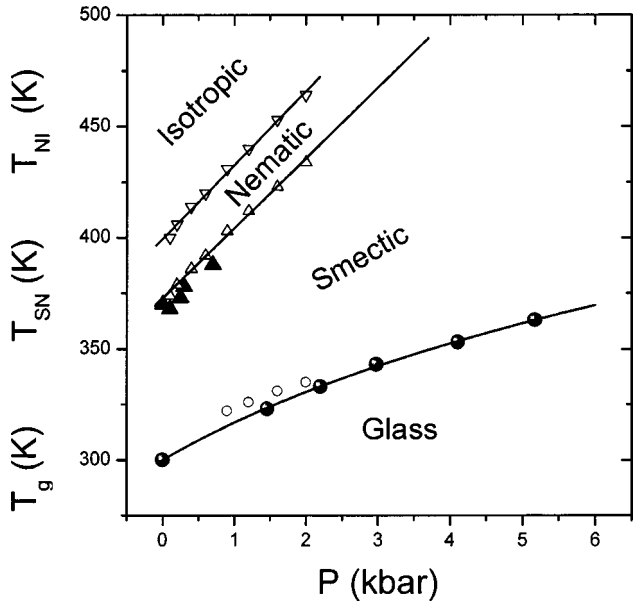

FIG. 10. Pressure dependence of the three characteristic temperatures: T_g (open and filled circles correspond to data obtained from the PVT and DS, respectively), T_{SN} (open and filled triangles correspond to data obtained from PVT and DS, respectively), and T_{NI} (open and filled inverse triangles correspond to data obtained from PVT and DS, respectively). The solid lines for the nematic-to-smectic and nematic-to-isotropic transitions are the result of linear fits to the PVT data (see text). Notice the stronger pressure dependence of the two first-order transitions. For the $T_g(P)$ dependence the line represents the result of the fit of the DS data to Eq. (7).

Figure 10, compares the pressure dependence of the three temperatures separating the four different regimes (glass-nematic-smectic-isotropic). In this respect, Fig. 10 serves as a phase diagram for the side-chain polymer liquid crystal sample. In the figure, both data from the PVT (open symbols) and DS (filled symbols) measurements are included for the T_g and T_{SN} transitions, however the T_{NI} transition could only followed by PVT. In DS, we have employed the results of Fig. 9 for the nematic-to-smectic transformation whereas for the $T_g(P)$ we have used the usual operational definition of T_g as the temperature corresponding to an α-process relaxation time of 100 s. Notice the good agreement between the static (PVT) and dynamic (DS) results for the two temperatures (T_g and T_{SN}) suggesting that the dynamic processes are directly coupled to the thermodynamic changes imposed by pressure. As expected, pressure affects more the two first order transitions as opposed to the, largely kinetic in origin, glass-to-liquid transformation. The latter can be fitted following the empirical equation [29]:

$$T_g(P) = c\left(1 + \frac{b}{a}P\right)^{1/b}, \tag{7}$$

where a, b, and c are fitting parameters. The solid line in Fig. 10 gives the result of the fit to the DS data alone with parameters $c = T_g(0) = 300$ K, $b = 5.7 \pm 0.05$, and $a = 15.7 \pm 0.5$ kbar. For the former transitions, the linear dependence can be rationalized in terms of the Clausius-Clapeyron equation

$$\frac{dP}{dT} = \frac{\Delta H}{T\Delta V}, \tag{8}$$

where ΔH is the latent heat associated with the smectic-to-nematic or nematic-to-isotropic transformation and ΔV is the associated volume change. Using the dP/dT value of 0.0319 kbar/K for the smectic-to-nematic transformation and the associated heat of fusion (2.5 J/g) from DSC, we obtain a change of volume of 2.1×10^{-3} cm^3/g at the transition. Due to the parallel behavior of the $T_{NI}(P)$ dependence, a similar volume change is also calculated for the nematic-to-isotropic transition. These estimates are in excellent agreement with the volume changes associated with both transitions from the PVT result (Fig. 3) as indicated in Table III.

Pressure can strongly influence the stability of the different mesophases. This results from the different P-dependence of the first order transitions among the mesophases and of the glass temperature. For example, the smectic mesophase is stable over 70 K at atmospheric pressure, but this range is doubled at 3 kbar. This brings forward a new possibility of control of the mesophase structure in liquid crystals; application of pressure results in a broader smectic mesophase within the P-T phase diagram. On the other hand, the stability of the nematic phase is less influenced by pressure due to the parallel $T_{SN}(P)$ and $T_{NI}(P)$ dependencies.

IV. CONCLUSIONS

Herein we investigated the structure and dynamics in a side chain polymer liquid crystal with a poly(methyl acrylate) backbone and a (*p*-alkoxy-phenyl)-benzoate mesogenic group. Three transition temperatures were identified separating the four equilibrium phases: glass, smectic, nematic, and isotropic. T and P were used in the study of the dynamics and the results have been compared with DSC and PVT measurements. Apart from the identification of the different dynamic processes we presented a complete phase diagram of the four phases within the T range from 300 to 470 K and for pressures in the range from 0.001 to 5 kbar. An excellent agreement was found between the static (PVT) and dynamic (DS) probes of the glass transition temperature as well as of the smectic-to-nematic transformation suggesting that the dynamics are coupled to the thermodynamic state of the system. Pressure exerts a strong influence on the melt mesophases by increasing the local order. As a consequence, increasing pressure results in a stable smectic mesophase over a larger temperature range.

ACKNOWLEDGMENT

We thank Mr. A. Best at MPI-P for the PVT measurements and for fruitful discussions.

[1] H. Finkelmann and G. Rehage, Adv. Polym. Sci. **60**, 99 (1984).
[2] V. P. Shibaev and N. A. Plate, Adv. Polym. Sci. **60**, 173 (1984).
[3] G. S. Attard, Mol. Phys. **58**, 1087 (1986).
[4] G. S. Attard, K. Arakia, and G. Williams, Br. Polym. J. **19**, 119 (1987).
[5] S. U. Vallerien, F. Kremer, and C. Boeffel, Liq. Cryst. **4**, 79 (1989).
[6] Ch. Cramer, Th. Cramer, F. Kremer, and R. Stannarius, J. Chem. Phys. **106**, 3730 (1997).
[7] S. A. Rozanski, F. Kremer, H. Groothues, and R. Stannarius, Mol. Cryst. Liq. Cryst. **303**, 319 (1997).
[8] A. Schönhals, D. Wolff, and J. Springer, Macromolecules **28**, 6254 (1995).
[9] A. Schönhals, D. Wolff, and J. Springer, Macromolecules **31**, 9019 (1998).
[10] J. Mijovic and J.-W. Sy, Macromolecules **33**, 9620 (2000).
[11] W. Heinrich and B. Stoll, Colloid Polym. Sci. **263**, 895 (1985).
[12] J. J. Moura-Ramos and G. Williams, Polymer **32**, 909 (1991).
[13] M. Mierzwa, G. Floudas, and A. Wewerka, Phys. Rev. E **64**, 031703 (2001).
[14] A. Wewerka, G. Floudas, T. Pakula, and F. Stelzer, Macromolecules **34**, 8129 (2001).
[15] M. Mierzwa, G. Floudas, and A. Wewerka, J. Non-Cryst. Solids **305**, 159 (2002).
[16] G. Rodekirch, J. Rübner, V. Zschuppe, D. Wolff, and J. Springer, Makromol. Chem. **194**, 1125 (1993).
[17] A. Schönhals and H.-E. Carius, Int. J. Polym. Mater. **45**, 239 (2000).
[18] S. Havriliak and S. Negami, Polymer **8**, 161 (1967).
[19] U. Pschorn, H. W. Spiess, B. Hisgen, and H. Ringsdorf, J. Makromol. Chem. **187**, 2711 (1985).
[20] G. Floudas, in *Broadband Dielectric Spectroscopy*, edited F. Kremer and A. Schönhals (Springer, Berlin, 2002), Chap. 8.
[21] G. Floudas and T. Reisinger, J. Chem. Phys. **111**, 5201 (1999).
[22] G. Floudas, C. Gravalides, T. Reisinger, and G. Wegner, J. Chem. Phys. **111**, 9847 (1999).
[23] G. Floudas, G. Fytas, T. Reisinger, and G. Wegner, J. Chem. Phys. **111**, 9129 (1999).
[24] M. Mierzwa, G. Floudas, P. Stepanek, and G. Wegner, Phys. Rev. B **62**, 14 012 (2000).
[25] M. Mierzwa and G. Floudas, IEEE Trans. Dielectr. Electr. Insul. **8**, 359 (2001).
[26] M. Paluch, A. Patkowski, and E. W. Fischer, Phys. Rev. Lett. **85**, 2140 (2000).
[27] B. D. Freeman, L. Bokobza, P. Sergot, L. Monnerie, and F. C. De Schryver, Macromolecules **23**, 2566 (1990).
[28] J. J. Fontanella, C. A. Edmondson, M. C. Wintersgill, Y. Wu, and S. G. Greenbaum, Macromolecules **29**, 4944 (1996).
[29] S. P. Andersson and O. Andersson, Macromolecules **31**, 2999 (1998).